Lattice Boltzmann Simulations of Karman Vortex Shedding from a Blunt Body in a Magnetic Fluid Flow

Y. Ido
Department of Engineering Physics, Electronics and Mechanics, Nagoya Institute of Technology, Japan
and M. Hata
Onomichi Dockyard Co., Ltd, Japan

Two dimensional lattice Boltzmann simulations are performed in order to investigate the magnetic fluid flow around a blunt body in the presence of magnetic field. Immersed boundary method is applied to describe the blunt circular cylinder in the flow. The magnetic fluid flow around a circular cylinder between the two parallel plates is simulated. We can control Karman vortex shedding form a blunt body in the magnetic fluid flow by applying magnetic field. The vortex shedding is suppressed by applying magnetic field induced from two magnets on the both sides of the wall near the blunt body. The lift force acting on the circular cylinder is increased when the magnet is arranged on one side of the wall near the cylinder.

Key Words: Magnetic fluid, Lattice Boltzmann method, Karman vortex, Vortex shedding, Flow control, Blunt body.

1. Introduction

The lattice Boltzmann method (LBM) is one of the useful simulation methods for calculating not only single phase flows but also multiphase flows [1-2]. The LBM is based on microscopic kinetic equations to calculate macroscopic behaviors of fluids. Various behaviors such as phase separation, surface deformation, cavitations, can be simulated by using the LBM. Some researchers have been reported behaviors of magnetic fluid by using the lattice Boltzmann method. Sofonea et al. [3-5] calculated two-dimensional interface deformation of a magnetic fluid droplet under uniform magnetic field and Hirabayashi et al. [6] analyzed the fractal structure of magnetic fluids in alternating magnetic field. Dellar simulated simple magnetic fluid flows with internal freedom [7]. The authors have reported the lattice Boltzmann simulations for deformation of interface between magnetic fluid and nonmagnetic fluid [8]. New additional term corresponding to the Maxwell stress tensor is introduced into the distribution function by the authors [9]. Some of basic flows of magnetic fluids have been analyzed, for example, simple shear flow between two parallel plates [10] and cavity flow [11]. However, even simple flows such as a flow around a blunt body have not been simulated as far as the authors know because it is difficult to deal with the magnetic interactions in magnetic fluids by using the ordinary Euler types of simulation method.

In this paper, we perform numerical simulations by using the hybrid method of lattice Boltzmann method [1,12] and the immersed boundary method [13-16] in order to investigate the magnetic fluid flows around a blunt body. In order to describe a circular cylinder in the flow, we use the immersed boundary method. Karman vortex shedding from a circular cylinder in magnetic fluid flows is computed by using this two-dimensional hybrid method and the effect of applied magnetic field is examined. Karman vortex shedding is one of important problems when blunt bodies are arranged in the flow field. In this study, force acting on the circular cylinder in a magnetic fluid flow is examined numerically.

Correspondence: Y. Ido, Department of Engineering Physics, Electronics and Mechanics, Nagoya Institute of Technology, Gokiso, Showa, Nagoya 466-8555, Japan
email: ido.yasushi@nitech.ac.jp

2. Simulation Method

2.1 LBM with immersed boundary method

In this study, we use the lattice Boltzmann method with immersed boundary method for simulating magnetic fluid flows. The lattice Boltzmann equation is given by

$$f_a(t+\Delta t, \boldsymbol{x}+\boldsymbol{c}_a\Delta t) = f_a(t,\boldsymbol{x}) - \frac{1}{\tau}\left[f_a(t,\boldsymbol{x}) - f_a^{eq}(t,\boldsymbol{x})\right] + \frac{3}{2}w_a \boldsymbol{F}\bullet\boldsymbol{c}_a, \quad (1)$$

where f_a is the distribution function of magnetic fluids in the ath direction at the position $\boldsymbol{x}$ and time

t, and $\boldsymbol{F}$ is the total force acting on the fluid particle. In our simulations, 2D9Q model is applied and $\boldsymbol{c}_a$ is the fluid particle velocity, where $a = 0$: zero velocity, $a = 1$, 2, 3 and 4: unit vectors to the left, up, right and down direction, $a = 5$, 6, 7 and 8: the vectors in the diagonal directions. In the above Eq. (1), the relaxation time is $\tau = 0.53$ in our simulations. The distribution function of 2D9Q model is described by the following equation:

$$f_a^{eq} = w_a \rho \left[1 + 3\boldsymbol{c}_a \bullet \boldsymbol{u} + \frac{9(\boldsymbol{c}_a \bullet \boldsymbol{u})^2}{2} - \frac{3\boldsymbol{u} \bullet \boldsymbol{u}}{2} \right], \quad (2)$$

where w_a is the weight function and w_0 = 4/9, $w_{1\sim4}$ = 1/9, and $w_{5\sim8}$ = 1/36. The macroscopic quantities such as the density and velocity are expressed by the following equations:

$$\rho = \sum_a f_a , \quad (3)$$

$$\boldsymbol{u} = \frac{1}{\rho} \sum_a f_a \boldsymbol{c} , \quad (4)$$

The total force $\boldsymbol{F}$ acting on the fluid particle is given by

$$\boldsymbol{F} = \sum_i \boldsymbol{F}_i^D + \boldsymbol{F}^M + \boldsymbol{F}^I , \quad (5)$$

where $\boldsymbol{F}_i^D$ is the magnetic dipole-dipole interaction force which acts on the target magnetic fluid particle with magnetic dipole moment $\boldsymbol{m}$ from the other magnetic fluid particle (magnetic dipole moment is $\boldsymbol{m}_i$ and the relative position vector from the target particle is $\boldsymbol{r}_i$). The magnetic moment is in the field direction and it is considered to be proportional to the applied magnetic field at the particle position. The dipole-dipole interaction force is expressed by

$$\boldsymbol{F}_i^D = \frac{3}{4\pi\mu_0 r_i^4} \left\{ (\boldsymbol{m} \bullet \boldsymbol{m}_i) \frac{\boldsymbol{r}_i}{r_i} - 5(\boldsymbol{m} \bullet \boldsymbol{r}_i)(\boldsymbol{m}_i \bullet \boldsymbol{r}_i) \times \frac{\boldsymbol{r}_i}{r_i^3} + \left[(\boldsymbol{m}_i \bullet \boldsymbol{r}_i)\boldsymbol{m} + (\boldsymbol{m} \bullet \boldsymbol{r}_i)\boldsymbol{m}_i \right] \frac{1}{r_i} \right\}, \quad (6)$$

The second term of the Eq. (5) is the magnetic force described by

$$\boldsymbol{F}^M = \boldsymbol{M} \bullet \nabla \boldsymbol{H} , \quad (7)$$

where $\boldsymbol{H}$ is the magnetic intensity vector and $\boldsymbol{M}$ is the magnetization of the magnetic fluid particle. The force $\boldsymbol{F}^I$ is the reaction force from the body in the flow and this force is calculated by using the immersed boundary method. A circular cylinder is described by the reference points on the circle. The force from the blunt body is given by

$$\boldsymbol{F}^I = \sum_b \boldsymbol{F}_b^I , \quad (8)$$

where $\boldsymbol{F}_b^I$ is the restoring force at the reference point b and it is defined by

$$\boldsymbol{F}_b^I = -k\boldsymbol{\xi}_b , \quad (9)$$

where $\boldsymbol{\xi}_b$ is the difference between the coordinate of the bth reference point and the equilibrium location of the bth reference point, k is the positive spring constant [17]. The constant k is determined by fitting the value of drag force and lift force acting on the circular cylinder in the absence of magnetic field (k=2.4 in our simulations). Thus, k is independent of magnetic field.

2.2 Analytical model

In our simulations, the flows of magnetic fluid around a circular cylinder are computed. Fig. 1 shows the analytical model. A circular cylinder is located at the center between two parallel plates. The size of the grid is 420 ×42 and the diameter of the circular cylinder is 10 grids. The circular cylinder is expressed by using the immersed boundary method and the cylinder is described by 126 reference points. The bounce-back condition is imposed in both parallel plates. We assume seven arrangements of the magnets: (A) no magnet, i.e., no magnetic field, (B) one magnet on one side of the wall, and (C) two magnets on both sides of the walls, and the magnets are located (a) upstream region, (b) near the cylinder and (c) downstream area, as shown in Fig. 1. The shift length of the position of the magnets is 100 Δx, where Δx is the size of the grid. In cases (C), combination of the magnetic poles of the magnets is (i) the same pole (N-N) and (ii) the different pole (N-S). Fig. 2 illustrates the distribution of magnetic field between the two parallel plates. We assume that the magnetization of the magnetic fluid particle

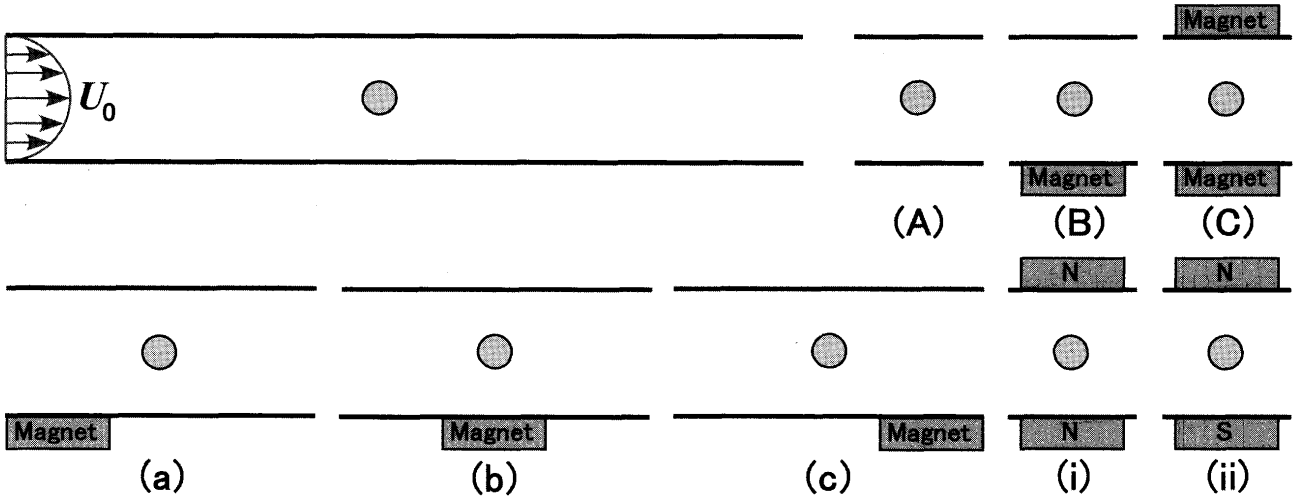

Fig. 1 Analytical model for the magnetic fluid flow around a circular cylinder. The flow between two parallel plates and the arrangement of the magnets is (A) no magnet, (B) one magnet on one side of the plate and (C) two magnets on both sides of the plates. The arrangement of the magnet is located (a) in the upstream region, (b) at the cylinder area, and (c) in the downstream region of the cylinder, respectively.

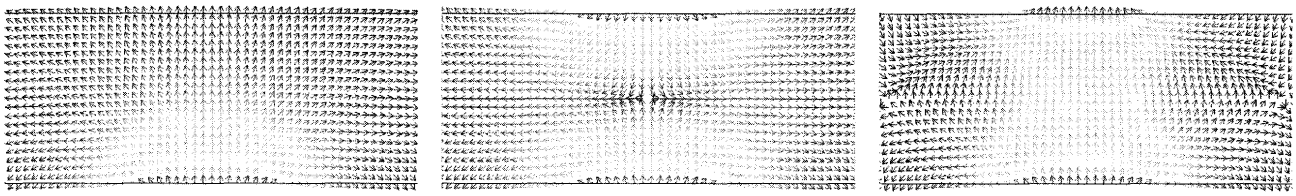

Fig. 2 Distribution of magnetic intensity vector between the parallel plates. (B) One magnet is located, and (C) two magnets are arranged on both sides of the plates. The pair of magnetic poles is (i) N-N and (ii) N-S.

is proportional to the magnetic field. The Poiseuille flow is given as the inflow condition (the maximum velocity is $U_0 = 0.1$) and outflow condition is the natural boundary condition. In this LBM simulation, kinetic viscosity is expressed by

$$\nu = \frac{1}{3}\left(\tau - \frac{1}{2}\right), \tag{10}$$

and the Reynolds number is $Re = U_0 d / \nu = 100$, where d is the diameter of the circular cylinder.

3. Results and Discussion

After 2×10^4 time steps, magnetic field is suddenly applied. Until just before applying magnetic field, Karman vortex street exists behind the circular cylinder. Fig. 3 shows the vorticity distribution of the flow field in the absence of magnetic field (no magnet is arranged) after 4×10^4 time steps. From this figure, typical Karman vortex shedding from the circular cylinder appears as usual Newtonian fluid flows. Figs. 4-6 demonstrate the vorticity distributions of the flow field after 4×10^4 time steps in the presence of magnetic field. From Fig. 6(b), twin vortices can be observed behind the circular cylinder, that is, there is no vortex shedding from the circular cylinder when the magnets are arranged on both sides of the plates near the circular cylinder with different pole facing each other. From Fig. 5(b), vortex shedding is suppressed when the magnets are arranged on both sides of the plates near the circular cylinder with the same pole facing each other. The Karman vortex shedding from the circular cylinder can be observed in other cases. This result indicates that it is important to arrange the magnets

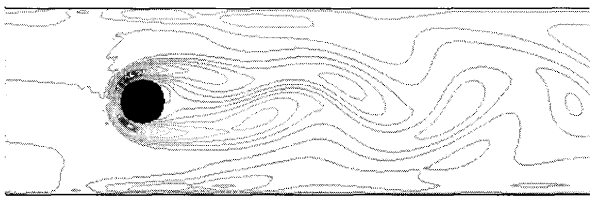

Fig. 3 Vorticity distribution of the flow field in the absence of magnetic field after 40000 time steps.

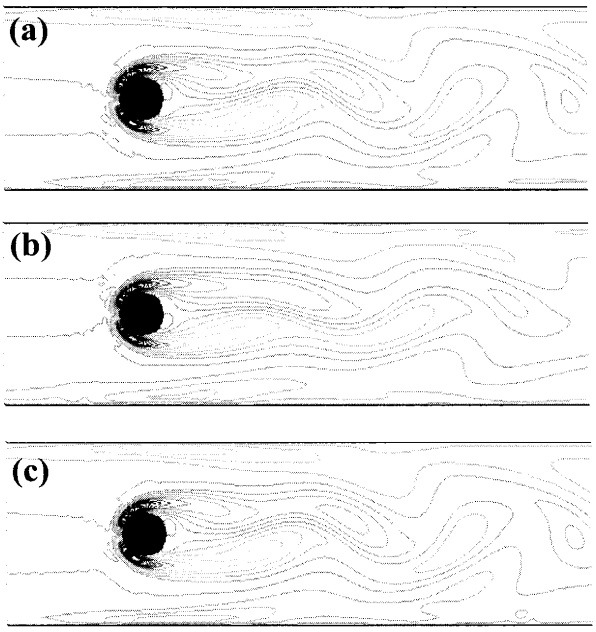

Fig. 4 Vorticity distributions of the flow field when one magnet is arranged on one side of the plate (Condition (B)) after 40000 time steps. The magnet is located in the (a) upstream region, (b) both sides of the cylinder, and (c) downstream region, respectively.

on both sides of the plates near the cylinder for reducing vortex shedding from the cylinder.

In order to verify the above result, the drag force and the lift force acting on the circular cylinder are calculated. Fig. 7 shows the drag coefficients C_D and Fig. 8 demonstrates the lift coefficients C_L, respectively. From Fig. 7, the drag force is decreased when the magnet or two magnets are located closely to the circular cylinder. The drag force in other cases is almost the same as the drag force acting on the cylinder in the absence of magnetic field. From Fig. 8, the lift force is increased in the arrangement of one magnet (B-1). In case (C-i), the amplitude of vibration of the lift force becomes small while the lift force does not act on the circular cylinder in case (C-ii). From Fig. 8, the lift force in case of (b) is different from that in other cases: variation of the lift force in other cases shows the same pattern. These results indicate that applying magnetic field in the narrowed area of the flow channel due to the existence of the circular cylinder is effective on control of the flow. As can be seen in Fig. 2, nonuniform magnetic field is induced from the magnet and the magnetic fluid particles are pulled to the magnet when one magnet is arranged on the plate or two magnets are located on both sides of the plates with the same pole facing each other. When

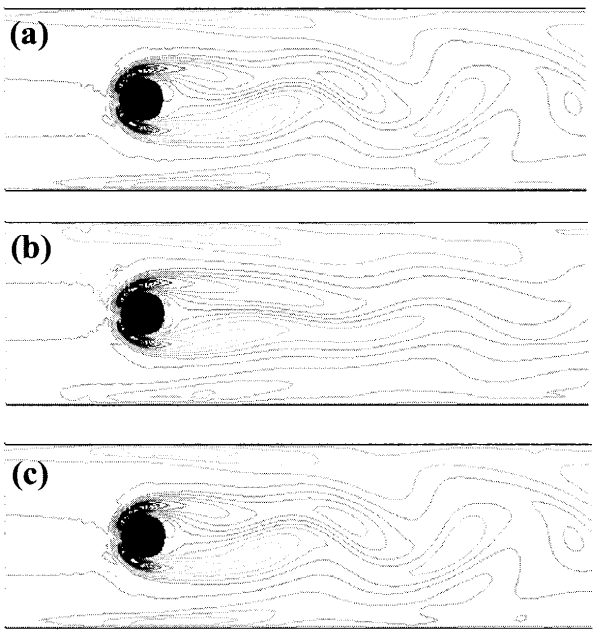

Fig. 5 Vorticity distribution of the flow field when two magnets are arranged on both sides of the plates and the same pole is facing each other (condition (C-i)) after 40000 time steps. Two magnets are located in the (a) upstream region, (b) both sides of the cylinder, and (c) downstream region, respectively.

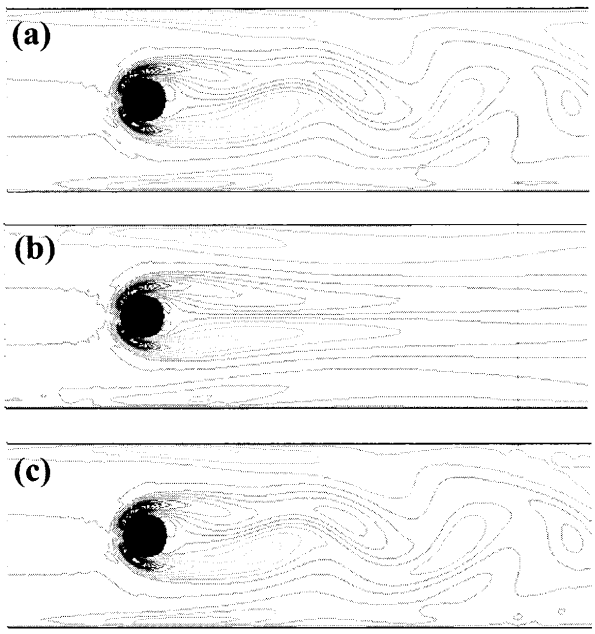

Fig. 6 Vorticity distribution of the flow field when two magnets are arranged on both sides of the plates and the different pole is facing each other (condition (C-ii)) after 40000 time steps. Two magnets are located in the (a) upstream region, (b) both sides of the cylinder, and (c) downstream region, respectively.

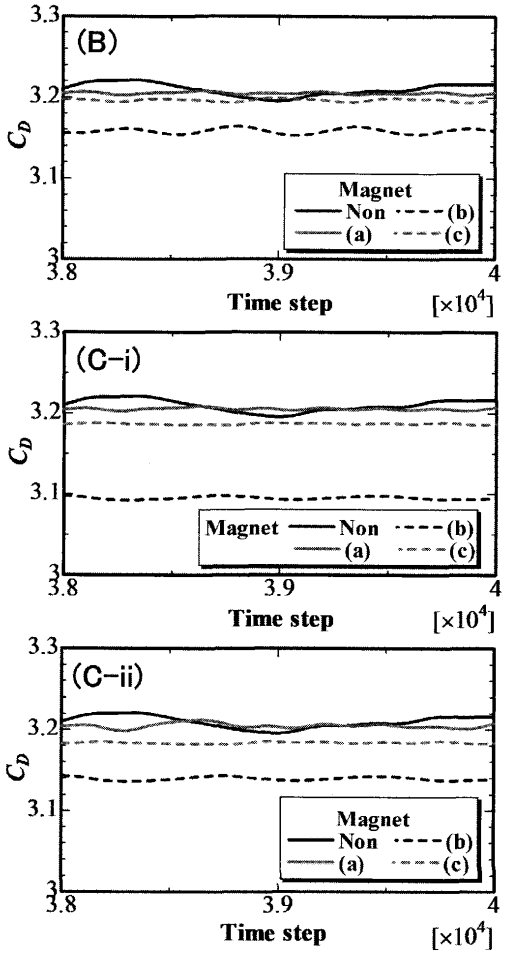

Fig. 7 The drag coefficients. (B) One magnet is arranged on one side of the plate and (C) two magnets are used. (i) The same pole is facing each other and (ii) different pole is facing each other. The magnet is located (a) upstream area, (b) near the cylinder, and (c) downstream area, respectively.

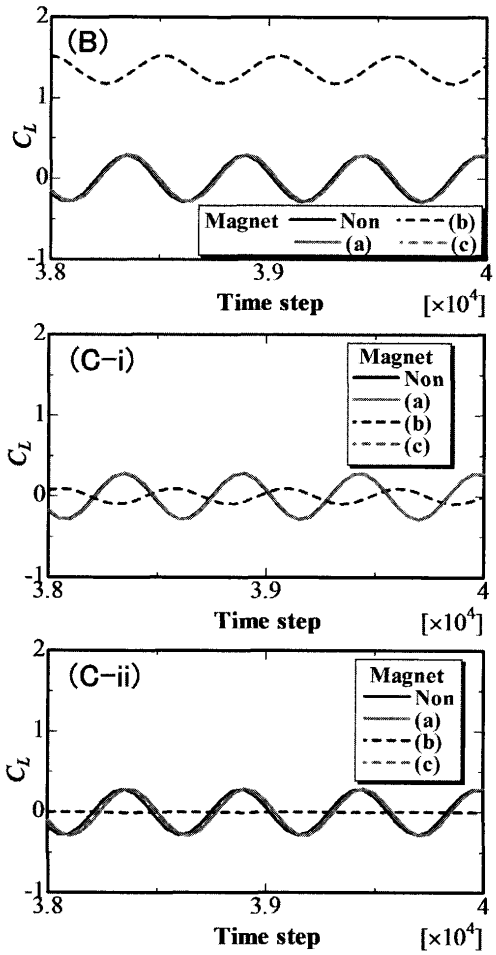

Fig. 8 The lift coefficients. (B) One magnet is arranged on one side of the plate and (C) two magnets are used. (i) The same pole is facing each other and (ii) different pole is facing each other. The magnet is located (a) upstream area, (b) near the cylinder, and (c) downstream area, respectively.

two magnets are on both sides of the plates with the different pole facing each other, magnetic flux connects between the magnets, thus, the magnetic dipole-dipole interaction force acts on the magnetic fluid particles in the direction between the magnets. Then the magnetic fluid particles are strongly interacted in the direction between the magnets just as the cluster formation of magnetic particles in magnetic fluids. Thus, the viscosity of the fluid is increased apparently, and both of the drag and the lift forces are reduced. Twin vortices appear behind the circular cylinder in the range of the Reynolds number $6 < Re < 40$, thus, the apparent viscosity in this case is more than 2.5 times of the viscosity in the absence of magnetic field. When the sensor stick is inserted in the flow pipe, it is possible to suppress vibration of the sensor stick due to the fluctuation of the lift force by applying magnetic field near the sensor.

4. Conclusion

We have performed two-dimensional lattice Boltzmann simulations with immersed boundary method in order to simulate the Karman vortex shedding from a circular cylinder in a magnetic fluid flow. It is found that the vortex shedding is suppressed and twin vortices appear behind the circular cylinder when two magnets are arranged on both sides of the two parallel plates near the cylinder. On the other hand, the lift force is increased when one magnet is located on one side of the plate near the circular cylinder.

References

[1] S. Chen and G. D. Doolen, "Lattice Boltzmann method for fluid flows," *Ann. Rev. Fluid Mech.*, Vol. 30, pp. 329-364, 1998.

[2] S. Succi, *The Lattice Boltzmann Equation for Fluid Dynamics and Beyond*, Oxford University Press, 2001.
[3] V. Sofonea, "Lattice Boltzmann approach to collective-particle interactions in magnetic fluids," *Europhys. Lett.*, Vol. 25, pp. 384-390, 1994.
[4] V. Sofonea and W. -G. Fruh, "Lattice Boltzmann model for magnetic fluid interfaces," *Euro. Phys. J. B*, Vol. 20, pp. 141-149, 2001.
[5] V. Sofonea, W. -G. Fruh and A. Cristea, "Lattice Boltzmann model for the simulation of interfacial phenomena in magnetic fluids," *J. Magn. Magn. Mat.*, Vol. 252, pp. 144-146, 2002.
[6] M. Hirabayashi, Y. Chen and H. Ohashi, "A new lattice Boltzmann approach to the fractal structure in magnetic fluids," *J. Magn. Magn. Mat.*, Vol. 252, pp. 138-140, 2002.
[7] J. Dellar, "Lattice Kinetic formulation for ferrofluids," *J. Statist. Phys.*, Vol. 121, pp. 105-118, 2005.
[8] Y. Ido, M. Yamanaka, M. Sasaki and T. Ozawa, "Lattice Boltzmann simulations of magnetic fluids under nonuniform magnetic field," *J. Jpn. Soc. Appl. Electro. Mech.*, Vol. 17, pp. 421-424, 2009.
[9] Y. Ido and M. Sasaki, "Three-dimensional Lattice Boltzmann simulations of a magnetic fluid drop under magnetic field," *Int. J. Appl. Electro. Mech.*, Vol. 33, pp. 1671-1676, 2010.
[10] Y. Ido and T. Tanahashi, "Fundamental theory for hydrodynamics of magnetic fluids," *Int. J. Appl. Electro. Mat.*, Vol. 3, pp. 183-191, 1992.
[11] H. Okanaga, K. Shizawa, N. Yashima and T. Tanahashi, "Numerical analysis of magnetic fluid flow in a dquare cavity: GSMAC finite element method of magnetic fluid," *Trans. Jpn. Soc. Mech. Eng.*, Vol. 53 B, pp. 2414-2422, 1987, (in Japanese).
[12] X. Shan and Y. Chen, "Lattice Boltzmann model for simulating flows with multiple phases and components," *Phys. Rev. E*, Vol. 47, pp. 1815-1819, 1993.
[13] R. Mittal, "Immersed boundary methods," *Ann. Rev. Fluid Mech.*, Vol. 37, pp. 239-261, 2005.
[14] P. Lallemand and L. Luo, "Lattice Boltzmann method for moving boundaries," *J. Comput. Phys.*, Vol. 184, pp. 406-421, 2003.
[15] A. J. C. Ladd, "Numerical simulations of particulate suspensions via a discretized Boltzmann equation. Part 2. Numerical results," *J. Fluid Mech.*, Vol. 271, pp. 311-339, 1994.
[16] Z-G. Feng and E. E. Michaelides, "Rhe immersed boundary-lattice Boltzmann method for solving fluid-particles interaction problems", *J. Comput. Phys.*, Vol. 195, pp. 602-628, 2004.

Received: 1 November 2010/Revised: 1 June 2011